ACS APPLIED ENERGY MATERIALS

www.acsaem.org Article

Nanochannel Engineering in Metal−Organic Frameworks by Grafting Sulfonic Groups for Boosting Proton Conductivity

Fan Yang, Ruimin Shi, Hongliang Huang,* Zhengqing Zhang, Xiangyu Guo, Zhihua Qiao, and Chongli Zhong

Cite This: *ACS Appl. Energy Mater.* 2022, 5, 3235−3241 Read Online

ACCESS | Metrics & More | Article Recommendations | Supporting Information

ABSTRACT: Constructing highly proton-conducting metal−organic frameworks (MOFs) remains a difficult challenge. Hence, we developed an effective nanochannel engineering strategy by grafting sulfonic-abundant benzene-1,3,5-trisulfonic acid (BTSA) onto the Zr_6-clusters of PCN-222 to act as a proton-conducting intensifier. Although the introduced BTSA dramatically reduced the pore volume, the resultant MOF (PCN-222-BTSA) exhibited strong water affinity and thus significantly enhanced water uptake at low RH values, reaching up to an almost equivalent water adsorption capacity at a high RH value compared with the capacity of pristine PCN-222. Benefiting from the enhanced water adsorption behavior and the proton-donating capability of sulfonic groups, PCN-222-BTSA displayed 2−3 orders of magnitude higher proton conductivity than pristine PCN-222. Our work is the first to report on postsynthetic modification in the nanochannel of MOFs for proton conduction, which demonstrates a strategy to design functional MOFs with abundant sulfonic groups and provides a bright avenue for constructing proton-conducting materials.

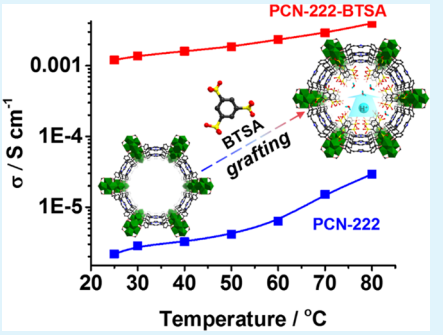

KEYWORDS: *benzene-1,3,5-trisulfonic acid, water adsorption, metal−organic framework, functionalization, proton conductivity*

INTRODUCTION

The usage of fossil fuels has caused severe environmental issues. Fuel cell (FC) technology provides a clean and efficient opportunity to alleviate the dependence on fossil fuels and thereby reduce carbon emissions.[1−3] However, electrolyte materials, which are critical for FCs, suffer from low proton conductivity, reducing the efficiency and increasing the costs of FCs.[4−6]

Most recently, due to their enormous structural diversity and functional tunability,[7−12] metal−organic frameworks (MOFs) have been drawing much attention as potential solid-state proton conductors, and various kinds of excellent MOFs have been successfully developed.[13,14] In general, the direct synthesis of new MOFs with a hydrophilic feature is the widespread method for designing and constructing proton-conducting MOFs. One of the most typical methods is the introduction of uncoordinated acidic groups into MOF channels.[15,16] For example, free carboxyl group-functionalized MIL-53(Fe)-$(COOH)_2$ exhibits the highest proton conductivity of 7.0×10^{-6} S cm^{-1} at 80 °C and 95% RH among the isostructural MIL-53 series MOFs.[17] In this system, the largest contribution to proton conductivity was found to be in good agreement with the pK_a values of the substituted benzoic acids, proving that the Bronsted-acid groups can boost the proton conductivity of MOFs. Correspondingly, UiO-66$(COOH)_2$ was also reported to exhibit a high proton conductivity of 2.3×10^{-3} S cm^{-1} at 90 °C and 95% RH.[18] The carboxyl groups in this MOF have a distinct role in enriching the water adsorption and simultaneously donate the protons, eventually enhancing the proton conductivity. Similar examples were also revealed in carboxyl group-functionalized BUT-83 and TJU-102.[19,20] In this manner, the MOFs with the free $-SO_3H$ group, which possesses stronger acidity than the carboxyl group, show much intensely improved proton conductivity, such as UiO-66-SO_3H and BUT-8(Cr)A.[21−23] However, owing to the uncontrollability of the coordination between metal ions and oxygen atoms of the acidic group, acidic groups are more easily deprotonated and thereby participate in the coordination reaction, resulting in serious changes in acidity and reducing the proton conductivity to much lower than expected. Up to now, only several MOFs with free $-SO_3H$ groups have been reported,[21,22] albeit the $-SO_3H$ group is regarded as one of the best groups for proton conduction. Therefore, new strategies for constructing MOFs with free acid groups, especially the $-SO_3H$ group, are highly desired.

Postsynthetic modification (PSM), which was first proposed by Robson in 1990[24] and first applied in MOFs by Cohen et

Received: December 7, 2021
Accepted: February 8, 2022
Published: February 21, 2022

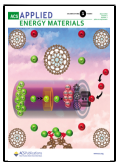

https://doi.org/10.1021/acsaem.1c03852
ACS Appl. Energy Mater. 2022, 5, 3235−3241

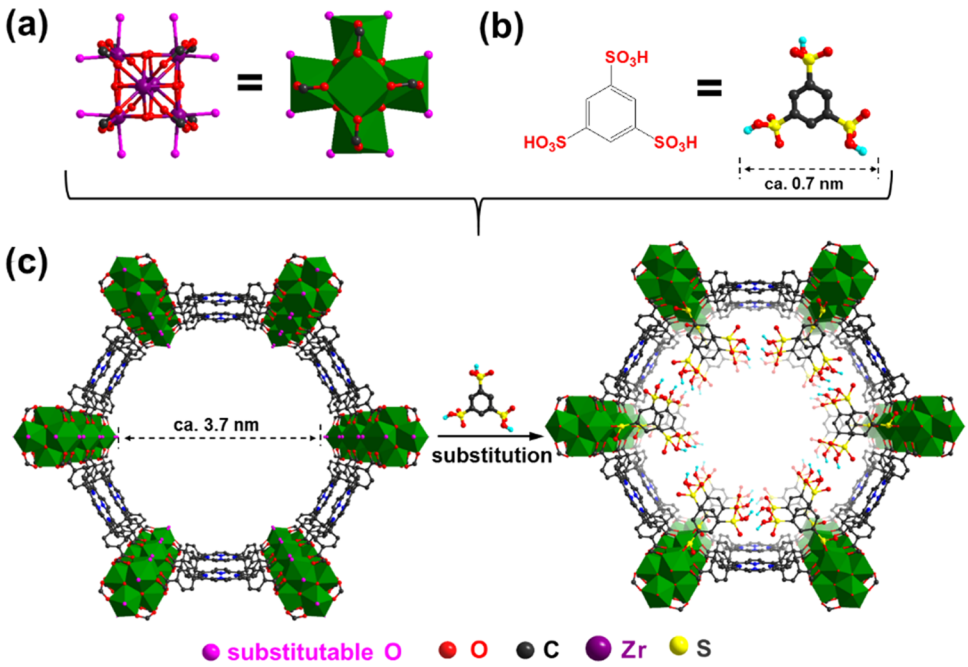

Figure 1. Schematic diagrams of functional PCN-222-BTSA. (a) Zr_6-cluster; (b) BTSA molecule; (c) proposed illustration of the substitution in the nanochannel of PCN-222-BTSA. Substitutable O, pink; other O, red; C, black; Zr, violet; S, yellow. Except for the hydrogen atoms of the sulfonic groups on BTSA, other hydrogen atoms are omitted for clarity.

al.,[25] extensively enlarges the designability of MOFs at the molecular level and expands the potentials of practical application. Although the PSM of MOFs has been widely adopted in gas adsorption and separation, catalysis, biomedicine, and sensing,[26−28] it is rare in augmenting proton conduction in MOFs. Loading guest materials with conductive properties into MOF channels is the most widely accepted PSM method. For example, the proton conductivity of MIL-101 could increase to 10^{-2} S cm^{-1} by introducing concentrated sulfuric acid or phosphoric acid into the pores.[29] Similarly, imidazoles,[30] triazoles,[31] and ionic liquids[32] can also be introduced into MOF channels as proton carriers to enhance proton or ionic conductivity. However, it is reasonable to deduce that the conductive guest materials may suffer a serious leakage owing to the lack of stable chemical bonds to immobilize them. Long-term use might thereby result in a sharp decrease in the proton conductivity. In addition, some guest materials such as sulfuric acid and phosphoric acid are highly corrosive, also affecting the stability of MOFs and even etching the components of PEMFCs. Despite these aforementioned methods, new PSM approaches to construct proton-conducting MOFs are still rare.[33−37] Therefore, it is necessary to develop advanced PSM methods to anchor functional groups and enhance proton conductivity.

Herein, we propose a rational strategy by introducing a sulfonic-group-abundant molecule, benzene-1,3,5-trisulfonic acid (BTSA), onto the Zr_6-cluster of PCN-222 to construct PCN-222-BTSA. XRD, FT-IR, XPS, and SEM were used to confirm the successful grafting of BTSA into PCN-222. Although BTSA sharply reduced the inner space of the MOF as revealed by N_2 uptake, the water absorption of PCN-222-BTSA effectively increased than that of PCN-222 at low RH, and saturated adsorption capacity was comparable to that of PCN-222 due to the strong water affinity of the introduced sulfonic groups. As expected, the proton conductivity of PCN-222-BTSA is 2 orders of magnitude higher than that of PCN-222 at all tested RH and temperatures. Especially, PCN-222-BTSA shows a conductivity of up to 4.0×10^{-3} S cm^{-1}, which is 136 times higher than that of PCN-222 at 80 °C and 100% RH. This work provides an effective way to construct more proton-conducting materials by introducing the functional groups through postsynthetic modifications.

EXPERIMENTAL SECTION

All chemicals were purchased from TCI and used without further purification.

Preparation of BTSA. BTSA was prepared by oxidizing benzene-1,3,5-trithiol in a H_2O_2 solution. Benzene-1,3,5-trithiol (871.7 mg, 5 mmol) was dispersed into the H_2O_2 (30 wt %, 20 mL) solution and stirred at room temperature for 48 h. The obtained mixture was slowly heated to 80 °C and kept for 6 h to decompose the residual H_2O_2. A gray solid was finally obtained by rotary evaporation.

Preparation of PCN-222 and PCN-222-BTSA. PCN-222 was prepared by the modified method described in the previous literature.[38] $ZrOCl_2 \cdot 8H_2O$ (2 g, 11.2 mmol) and tetrakis(4-carboxyphenyl)porphyrin (TCPP, 0.4 g, 0.5 mmol) were quickly added to the mixture of anhydrous DMF (500 mL) and formic acid (300 mL) in a round bottom flask and then heated to 135 °C and kept for 80 h. After cooling down to room temperature, a purple powder was obtained by centrifugation. Then, the obtained powder was thoroughly washed with *N*,*N*-dimethylformamide (DMF) and acetone and dried at 100 °C for further use.

PCN-222-BTSA was prepared by functionalizing PCN-222 with BTSA. After being fully dried at vacuum, the activated PCN-222 (0.2 g) was added to 10 mL of 0.5 mol L^{-1} BTSA/DMF solution and heated at 80 °C for 24 h. A green precipitate was collected by centrifugation and washed with DMF methanol three times and then immersed in methanol five times to exchange DMF and residual BTSA in the pores. Finally, after centrifugation and drying at 80 °C overnight, the green PCN-222-BTSA was obtained.

Characterizations. Powder X-ray diffraction (PXRD) patterns were obtained on a Bruker D2 PHASER XRD with powder samples (Cu Kα radiation, λ = 0.1541874). N_2 adsorption−desorption isotherms were collected at 77 K using a Micromeritics ASAP 2020 device. Water uptakes were measured in a Microtrac BELSORP MAX

https://doi.org/10.1021/acsaem.1c03852
ACS Appl. Energy Mater. 2022, 5, 3235−3241

instrument. The sample morphology was recorded using a GeminiSEM 500 scanning electron microscope (SEM). FT-IR spectra of all samples were recorded using a Thermo Nicolet 380 spectrometer with pressed KBr pellets under the wavenumber within the range of 400−4000 cm^{-1}. An X-ray photoelectron spectrometer (XPS) (Al Kα radiation at 1486.6 eV NEXSA, Thermo Scientific) was used to analyze electronic properties. ^{1}H NMR spectra were recorded using a Bruker Fourier 600M spectrometer. A vario EL cube was used to measure the S content in PCN-222-BTSA.

Proton Conductivity Test. The proton conductivity tests were operated similarly to our previous work.[21,22] A powder material was pressed into a cuboid pellet (1 cm × 0.4 cm × l, where l is the thickness of the pellet, cm, used for proton conductivity test at 100% RH) or cylinder pellet (0.6 cm in diameter, where l is the thickness of the pellet, cm, used for proton conductivity test at 33−85% RH) at a pressure of 1000 kg cm^{-2} for 2 min. Both sides of the pellet were attached to silver wires with silver paste and sealed in a homemade glass chamber. The relative humidity was controlled with a saturated salt solution. The alternating current (a.c.) impedance plots were recorded at a CHI760E electrochemical workstation with a frequency range of 1 Hz to 1 MHz at 25−80 °C and a disturbance voltage of 100 mV.

The proton conductivity (σ, S cm^{-1}) was calculated according to the following equation (l, thickness, cm; R, impedance, Ω; S, the area of the pellet, cm^2)

$$\sigma = l/(RS) \quad (1)$$

The activation energy (E_a) was estimated by the Arrhenius equation

$$\sigma T = \exp(-E_a/k_B T) \quad (2)$$

where k_B (J K^{-1}) is the Boltzmann constant and T (K) is the temperature.

RESULTS AND DISCUSSION

PCN-222 is a highly stable Zr-MOF consisting of Zr_6 clusters and tetrakis(4-carboxyphenyl) porphyrin ligands.[38] There exists eight terminal −OH groups coordinated on the Zr_6-cluster (Figure 1a), which can be substituted by oxygen atoms in some oxygen-containing groups,[39] such as sulfuric acid[40] and $-PO_3H_2$ groups.[41] Meanwhile, the BTSA molecule was ∼0.7 nm, obviously much smaller than the diameter of one-dimensional nanochannels (ca. 3.7 nm) in PCN-222. It is reasonable to deduce that such large channels of PCN-222 favor the free entry of BTSA, implying the feasibility of this grafting strategy. Therefore, both the Zr_6-cluster with substitutable OH groups and the larger pores in PCN-222 provide an opportunity to graft the BTSA by substitution reactions.

To fabricate PCN-222-BTSA, BTSA was successfully prepared by oxidizing benzene-1,3,5-trithiol in a H_2O_2 solution (Scheme 1), which can be proved by ^{1}H NMR spectrogram (Figure S1). After stirring the mixture of BTSA and PCN-222 in DMF at 80 °C, PCN-222-BTSA was finally obtained, and its PXRD pattern matched well with that of the pristine PCN-222 (Figure S2), implying that this graft strategy did not change the main structure of PCN-222 due to the high stability of this MOF. Further, the XPS spectra of S 2s and S 2p signals suggest the successful grafting of BTSA into PCN-222 nanochannels (Figure 2a). Most importantly, Zr 3d XPS spectra clearly showed an evident shift, strongly proving the coordination between the Zr atoms of Zr_6 clusters and the O atoms of the sulfonate groups (Figure 2b). Moreover, the FT-IR spectra exhibit the typical characteristic peaks at 1240 and 603 cm^{-1}, which are separately assigned to the S═O and C−S vibrations of BTSA, still revealing the grafted BTSA anchored in the nanochannels (Figure 2c). PCN-222, however, does not possess these BTSA features in its XPS and FT-IR spectra. Meanwhile, the SEM images show that the morphology of PCN-222-BTSA is needlelike, which is in agreement with pristine PCN-222 (Figure S3), proving that this MOF maintained its structural integrity during the grafting procedure due to the high stability of PCN-222. The elemental mapping also clearly demonstrates that the element sulfur disperses uniformly in the sample, indicating the well-dispersed sulfonic groups of BTSA in PCN-222-BTSA (Figure 2d−f). According to the EA and EDS results, the contents of element sulfur in PCN-222-BTSA were 12.22 and 11.93 wt %, respectively, which means there are about five BTSA per Zr_6 cluster in PCN-222-BTSA. In brief, combining the results of the PXRD patterns, XPS spectra, FT-IR spectra, and SEM images and its mapping, we fully prove that the BTSA molecule is uniformly grafted onto the Zr_6 clusters by coordination interactions, and the PCN-222-BTSA is successfully obtained.

To investigate the contribution of the introduced BTSA to the adsorption property, which is important for proton conductivity, the N_2 and water vapor uptake tests were conducted. As shown in Figure 3a, the surface area of PCN-222-BTSA was discovered to be only 451 m^2 g^{-1}, which is sharply decreased compared to that of PCN-222 (2245 m^2 g^{-1}). This fact evidently reveals the BTSA anchors on the Zr_6-clusters and thereby reduces the inner space of this MOF, which is in good agreement with the aforementioned characterization analyses. Surprisingly, however, the water uptakes of PCN-222-BTSA are much higher than those of PCN-222 below 75% RH. For example, the water uptake of PCN-222-BTSA at 33% RH was 190 cm^3 g^{-1}, 2.7 times higher than that of PCN-222 (71 cm^3 g^{-1}) at such a condition. The prominent enhancement of water uptake of PCN-222-BTSA may be reasonably explained by the high hydrophilicity of sulfonic groups, which benefit the water adsorption. Although the inner space of the PCN-222-BTSA pore is partially occupied by BTSA, the strong affinity of these introduced sulfonic groups on BTSA significantly enhances the water uptake and eventually leads to the high water uptake capacity at a high RH (>75%) condition, which is comparable to that of PCN-222. The DFT-calculated binding energy of water in PCN-222-BTSA was 51.17 kJ mol^{-1}, obviously higher than that in the PCN-222 (44.46 kJ mol^{-1}, Figure S4). The higher binding energy is in good agreement with the higher water adsorption amount in PCN-222-BTSA, strongly proving the higher water affinity of PCN-222-BTSA. This unique water uptake behavior of the PCN-222-BTSA may be in favor of forming much denser hydrogen-bonding networks, contributing to a more smooth proton migration pathway, as discussed below.

To uncover the contribution of the introduced sulfonic groups on the proton conductivity, the a.c. impedance experiments were performed. Random impedance signals of PCN-222 were detected below 75% RH, which implies that the impedance is too large to be detected due to the poor proton

Scheme 1. Synthetic Route of the BTSA Molecule

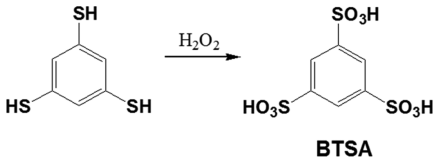

https://doi.org/10.1021/acsaem.1c03852
ACS Appl. Energy Mater. 2022, 5, 3235−3241

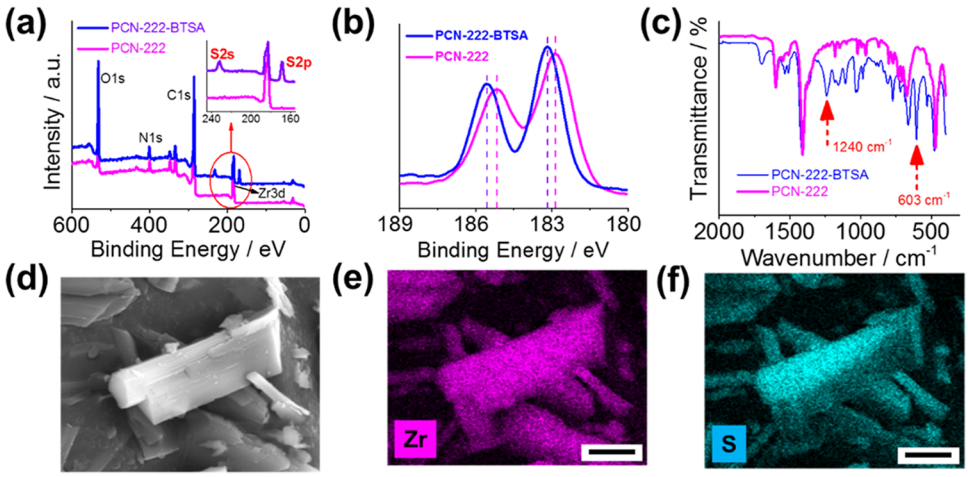

Figure 2. Characteristics of PCN-222-BTSA. (a, b) XPS spectra of PCN-222-BTSA and PCN-222; (c) FT-IR spectra of PCN-222-BTSA, PCN-222, and BTSA; (d–f) SEM and mapping images of PCN-222-BTSA. Scale bar: 5 μm.

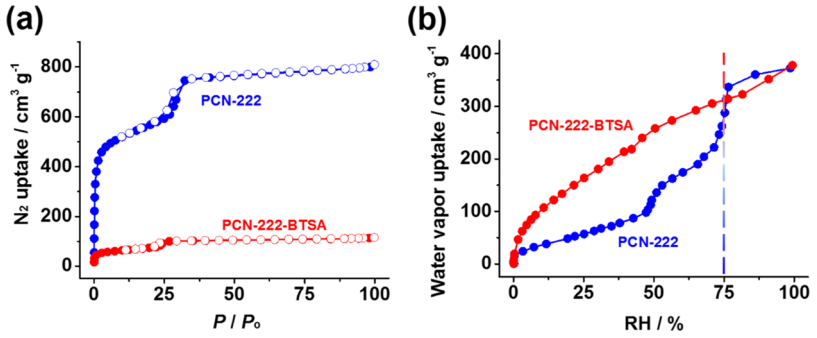

Figure 3. Gas uptake isotherms of PCN-222-BTSA and PCN-222: (a) N_2 and (b) H_2O vapor. Open symbol, adsorption; closed symbol, desorption.

conductivity at such a low RH. Even at a high RH, the Nyquist plots of PCN-222 are really rough and just barely meet the evaluation of proton conductivity (Figure S6). On the contrary, however, PCN-222-BTSA shows perfect and smooth Nyquist plots, which could be well fitted with the proposed equivalent circuit regardless of whether the RH is low or high (Figures 4a–c, S4, and S5). After calculating using eq 1, the proton conductivities of PCN-222-BTSA were found to dramatically increase with the elevated RH, which is remarkably higher than that of PCN-222 at all RHs (Figure 4d). For instance, the proton conductivity of PCN-222-BTSA at 75% RH was 3.8×10^{-5} S cm^{-1}, 959-fold higher than that of PCN-222, which is only 4.0×10^{-8} S cm^{-1}, although the water adsorption capacity values of PCN-222-BTSA and PCN-222 at this RH are almost close to each other. Moreover, the conductivity of PCN-222-BTSA at 33% RH was 2.0×10^{-7} S cm^{-1}, even higher than that of the PCN-222 at 85% RH. These results strongly prove that the BTSA significantly improves the proton conductivity, which is in good agreement with the different water adsorption behaviors before and after BTSA modifications.

To further unlock the proton transport mechanism, temperature-dependent Nyquist plots were constructed at 100% RH. Both PCN-222-BTSA and PCN-222 show neat semicircles, implying that both materials can conduct protons. However, PCN-222-BTSA obviously showed a much smaller semicircle than PCN-222, indicating that the resistance of the PCN-222-BTSA pellet is very small (Figure 5a,b). Therefore,

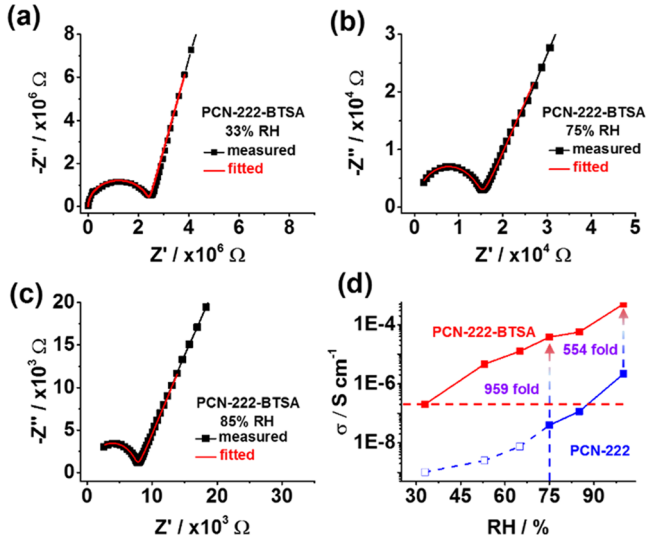

Figure 4. (a–c) Measured and fitted Nyquist plots of PCN-222 at different RH values: (a) 33% RH, (b) 75% RH, and (c) 85% RH. (d) Humidity-dependent proton conductivity of PCN-222-BTSA and PCN-222 at 25 °C and different RH values. Hollow squares represent almost undetected proton conductivity of PCN-222 below 75% RH.

the proton conductivities of PCN-222-BTSA were revealed to be outstandingly higher than those of PCN-222 at all tested temperatures (Figure 5c). For example, the proton conductivity of PCN-222-BTSA was 1.4×10^{-3} S cm^{-1} at 30 °C,

https://doi.org/10.1021/acsaem.1c03852
ACS Appl. Energy Mater. 2022, 5, 3235–3241

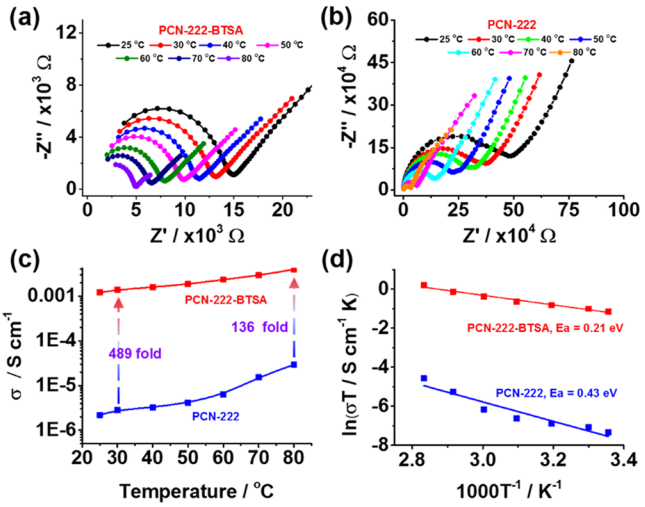

Figure 5. (a) Temperature-dependent Nyquist plots of PCN-222-BTSA at 100% RH; (b) temperature-dependent Nyquist plots of PCN-222 at 100% RH; (c) proton conductivity of PCN-222-BTSA and PCN-222 at 100% RH and different temperatures; (d) E_a of PCN-222-BTSA and PCN-222.

489-fold higher than that of PCN-222, for which it is only 2.8 × 10^{-6} S cm^{-1}. As the temperature increased to 80 °C, the proton conductivity of PCN-222-BTSA increased to 4.0 × 10^{-3} S cm^{-1}, still 2 orders of magnitude higher than that of PCN-222. This proton conductivity of PCN-222-BTSA is higher than that of some typical MOFs, such as 1,2,3-triazole@$Cu_2(F_2AzoBDC)_2(dabco)$ (1.2 × 10^{-4} S cm^{-1}),[42] UiO-$66(COOH)_2$ (2.3 × 10^{-3} S cm^{-1}),[18] UiO-66-SO_3H (3.4 × 10^{-3} S cm^{-1}),[21] and $Fe(OH)(bdc\text{-}(COOH)_2)$ (2.0 × 10^{-6} S cm^{-1}),[17] proving that our nanochannel engineering strategy is effective to enhance the proton conductivity. These data convincingly prove that the BTSA can effectively promote the proton conductivity of PCN-222. Moreover, PCN-222-BTSA can maintain its conductivity (Figure S8) and structural integrity (Figure S2) after 100 h, demonstrating excellent stability. Furthermore, the proton-conducting E_a of PCN-222-BTSA was found to be 0.21 eV according to eq 2 (Figure 5d), implying that the proton transport behavior in this material follows the Grotthuss mechanism. But, the E_a of PCN-222 was 0.43 eV, which is much higher than that of PCN-222-BTSA, indicating that the proton is hard to migrate due to lack of sulfonic groups.

Based on the abovementioned structural features and proton conductivity analyses, we propose a possible model to reasonably explain the proton-conducting pathway (Figure 6). As clearly demonstrated in the literature,[43] hydrogen bonds are responsible for the proton migration, which follows the Grotthuss mechanism. It is no doubt that the hydrogen bonds could form between the water molecules and the hydrophilic atoms/groups, including the carboxylic acid group at the MOF terminal in both PCN-222-BTSA and PCN-222. However, for PCN-222-BTSA, the strong water affinity of $-SO_3H$ groups improves its water adsorption, which benefits the formation of dense hydrogen-bonding networks, offering a smooth pathway for proton transportation at both low and high RH values. For PCN-222, a successive hydrogen-bonding network is hard to be formed in such large pores due to the lack of functional $-SO_3H$ groups, leading to low proton conductivity. Therefore, the proton would be much easy to conduct by the dense

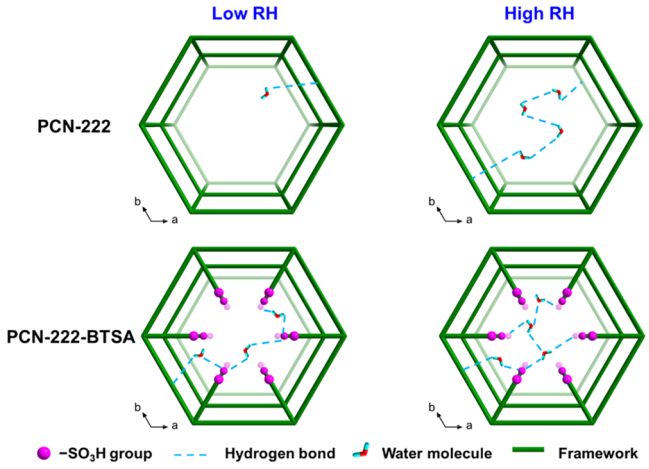

Figure 6. Proposed hydrogen bonds in the 1D channels along the *c* axis in PCN-222-BTSA and PCN-222.

hydrogen-bonding networks along *the c* axis in PCN-222-BTSA than in PCN-222. Moreover, regardless of whether the RH value is low or high, the $-SO_3H$ group could donate protons in the water-containing channels, which also enhances the proton conductivity of PCN-222-BTSA. Hence, at all investigated RH values and temperatures, the proton conductivity of PCN-222-BTSA is at least 2−3 orders of magnitudes higher than that of PCN-222, indicating that the BTSA modification strategy could significantly enhance proton conduction.

CONCLUSIONS

In summary, we developed a rational nanochannel engineering strategy to construct proton-conducting PCN-222-BTSA with abundant $-SO_3H$ groups by introducing BTSA molecules onto the Zr_6 clusters of PCN-222. The introduced $-SO_3H$ groups in the resultant PCN-222-BTSA enhanced the water adsorption, which benefited the formation of successive hydrogen-bonding networks at both low RH and high RH, leading to the proton conductivity 2−3 orders of magnitude higher than that of pristine PCN-222 at all evaluated RHs and temperatures. To the best of our knowledge, PCN-222-BTSA is the first postsynthetic modification of the nanochannel in MOFs for proton conduction, thus opening a new avenue to construct MOFs and other materials with high proton conductivity.

ASSOCIATED CONTENT

Supporting Information

The Supporting Information is available free of charge at https://pubs.acs.org/doi/10.1021/acsaem.1c03852.

DFT calculation details of water-binding energy in PCN-222-BTSA and PCN-222 and experimental details including the ^1H NMR spectrum for BTSA; PXRD patterns for all compounds; SEM images for PCN-222; an equivalent circuit used for fitting all of the Nyquist plots; and the fitted Nyquist plots of PCN-222-BTSA and PCN-222 at different RH values (PDF)

AUTHOR INFORMATION

Corresponding Author

Hongliang Huang − *State Key Laboratory of Separation Membranes and Membrane Processes, Tiangong University,*

https://doi.org/10.1021/acsaem.1c03852
ACS Appl. Energy Mater. 2022, 5, 3235−3241

Tianjin 300387, P. R. China; School of Chemical Engineering and Technology, Tiangong University, Tianjin 300387, P. R. China; orcid.org/0000-0001-9690-9259; Email: huanghongliang@tiangong.edu.cn

Authors

Fan Yang − *State Key Laboratory of Separation Membranes and Membrane Processes, Tiangong University, Tianjin 300387, P. R. China; School of Chemical Engineering and Technology, Tiangong University, Tianjin 300387, P. R. China*

Ruimin Shi − *State Key Laboratory of Separation Membranes and Membrane Processes, Tiangong University, Tianjin 300387, P. R. China; School of Chemical Engineering and Technology, Tiangong University, Tianjin 300387, P. R. China*

Zhengqing Zhang − *State Key Laboratory of Separation Membranes and Membrane Processes, Tiangong University, Tianjin 300387, P. R. China; School of Chemical Engineering and Technology, Tiangong University, Tianjin 300387, P. R. China;* orcid.org/0000-0003-2403-1461

Xiangyu Guo − *State Key Laboratory of Separation Membranes and Membrane Processes, Tiangong University, Tianjin 300387, P. R. China; School of Chemical Engineering and Technology, Tiangong University, Tianjin 300387, P. R. China;* orcid.org/0000-0001-9794-5286

Zhihua Qiao − *State Key Laboratory of Separation Membranes and Membrane Processes, Tiangong University, Tianjin 300387, P. R. China; School of Chemical Engineering and Technology, Tiangong University, Tianjin 300387, P. R. China*

Chongli Zhong − *State Key Laboratory of Separation Membranes and Membrane Processes, Tiangong University, Tianjin 300387, P. R. China; School of Chemical Engineering and Technology, Tiangong University, Tianjin 300387, P. R. China;* orcid.org/0000-0002-7921-9923

Complete contact information is available at: https://pubs.acs.org/10.1021/acsaem.1c03852

Notes

The authors declare no competing financial interest.

■ ACKNOWLEDGMENTS

This work was supported by the National Natural Science Foundation of China (Nos. 22038010, 22008181, 22008179, 21978212, 22108202, and 22122810) and the Science and Technology Plans of Tianjin (Nos. 20ZYJDJC00110 and 21ZYJDJC00040). The authors thank the Analytical & Testing Center of Tiangong University.

■ REFERENCES

(1) *Fuel Cell Technologies Office: Multi-Year Research, Development, Demonstration Plan. 3.4. Technical Plan-Fuel Cells*; U.S. Department of Energy, 2012.

(2) Liang, Z.; Qu, C.; Guo, W.; Zou, R.; Xu, Q. Pristine Metal−organic Frameworks and Their Composites for Energy Storage and Conversion. *Adv. Mater.* **2018**, *30*, No. 1702891.

(3) Li, X.-M.; Dong, L.-Z.; Li, S.-L.; Xu, G.; Liu, J.; Zhang, F.-M.; Lu, L.-S.; Lan, Y.-Q. Synergistic Conductivity Effect in a Proton Sources-Coupled Metal−organic Framework. *ACS Energy Lett.* **2017**, *2*, 2313−2318.

(4) Wahiduzzaman, M.; Wang, S.; Schnee, J.; Vimont, A.; Ortiz, V.; Yot, P. G.; Retoux, R.; Daturi, M.; Lee, J. S.; Chang, J.-S.; Serre, C.; Maurin, G.; Devautour-Vinot, S. A High Proton Conductive Hydrogen-Sulfate Decorated Titanium Carboxylate Metal−Organic Framework. *ACS Sustainable Chem. Eng.* **2019**, *7*, 5776−5783.

(5) Koseki, K.; Arita, T.; Tabata, K.; Nohara, T.; Sato, R.; Nagano, S.; Masuhara, A. Effect of Surface Silanol Density on the Proton Conductivity of Polymer-Surface-Functionalized Silica Nanoparticles. *ACS Sustainable Chem. Eng.* **2021**, *9*, 10093−10099.

(6) Hickner, M. A.; Ghassemi, H.; Kim, Y. S.; Einsla, B. R.; McGrath, J. E. Alternative Polymer Systems for Proton Exchange Membranes (PEMs). *Chem. Rev.* **2004**, *104*, 4587−4611.

(7) Wang, B.; He, R.; Xie, L.-H.; Lin, Z.-J.; Zhang, X.; Wang, J.; Huang, H.; Zhang, Z.; Schanze, K. S.; Zhang, J.; Xiang, S.; Chen, B. Microporous Hydrogen-Bonded Organic Framework for Highly Efficient Turn-Up Fluorescent Sensing of Aniline. *J. Am. Chem. Soc.* **2020**, *142*, 12478−12485.

(8) Devautour-Vinot, S.; Maurin, G.; Serre, C.; Horcajada, P.; Cunha, D. P.; Guillerm, V.; Costa, E. S.; Taulelle, F.; Martineau, C. Structure and Dynamics of the Functionalized MOF Type UiO-66(Zr): NMR and Dielectric Relaxation Spectroscopies Coupled with DFT Calculations. *Chem. Mater.* **2012**, *24*, 2168−2177.

(9) He, T.; Kong, X.-J.; Li, J.-R. Chemically Stable Metal−Organic Frameworks: Rational Construction and Application Expansion. *Acc. Chem. Res.* **2021**, *54*, 3083−3094.

(10) Duan, C.; Yu, Y.; Xiao, J.; Li, Y.; Yang, P.; Hu, F.; Xi, H. Recent Advancements in Metal−Organic Frameworks for Green Applications. *Green Energy Environ.* **2021**, *6*, 33−49.

(11) He, T.; Huang, Z.; Yuan, S.; Lv, X.-L.; Kong, X.-J.; Zou, X.; Zhou, H.-C.; Li, J.-R. Kinetically Controlled Reticular Assembly of a Chemically Stable Mesoporous Ni(II)-Pyrazolate Metal−Organic Framework. *J. Am. Chem. Soc.* **2020**, *142*, 13491−13499.

(12) Pattengale, B.; Ostresh, S.; Schmuttenmaer, C. A.; Neu, J. Interrogating Light-Initiated Dynamics in Metal−Organic Frameworks with Time-Resolved Spectroscopy. *Chem. Rev.* **2021**, *121*, 13238−13341.

(13) Ye, Y.; Gong, L.; Xiang, S.; Zhang, Z.; Chen, B. Metal−Organic Frameworks as a Versatile Platform for Proton Conductors. *Adv. Mater.* **2020**, *32*, No. 1907090.

(14) Lim, D.-W.; Kitagawa, H. Proton Transport in Metal−Organic Frameworks. *Chem. Rev.* **2020**, *120*, 8416−8467.

(15) Bhadra, B. N.; Ahmed, I.; Lee, H. J.; Jhung, S. H. Metal−Organic Frameworks Bearing Free Carboxylic Acids: Preparation, Modification, and Applications. *Coord. Chem. Rev.* **2022**, *450*, No. 214237.

(16) Xie, X.-X.; Yang, Y.-C.; Dou, B.-H.; Li, Z.-F.; Li, G. Proton Conductive Carboxylate-Based Metal−Organic Frameworks. *Coord. Chem. Rev.* **2020**, *403*, No. 213100.

(17) Shigematsu, A.; Yamada, T.; Kitagawa, H. Wide Control of Proton Conductivity in Porous Coordination Polymers. *J. Am. Chem. Soc.* **2011**, *133*, 2034−2036.

(18) Borges, D. D.; Devautour-Vinot, S.; Jobic, H.; Ollivier, J.; Nouar, F.; Semino, R.; Devic, T.; Serre, C.; Paesani, F.; Maurin, G. Proton Transport in a Highly Conductive Porous Zirconium-Based Metal−Organic Framework: Molecular Insight. *Angew. Chem., Int. Ed.* **2016**, *55*, 3919−3924.

(19) Wu, H.; Yang, F.; Lv, X. L.; Wang, B.; Zhang, Y. Z.; Zhao, M. J.; Li, J.-R. A Stable Porphyrinic Metal−Organic Framework Pore-Functionalized by High-Density Carboxylic Groups for Proton Conduction. *J. Mater. Chem. A* **2017**, *5*, 14525−14529.

(20) Tian, Y.; Liang, G.; Fan, T.; Shang, J.; Shang, S.; Ma, Y.; Matsuda, R.; Liu, M.; Wang, M.; Li, L.; Kitagawa, S. Grafting Free Carboxylic Acid Groups onto the Pore Surface of 3D Porous Coordination Polymers for High Proton Conductivity. *Chem. Mater.* **2019**, *31*, 8494−8503.

(21) Yang, F.; Huang, H.; Wang, X.; Li, F.; Gong, Y.; Zhong, C.; Li, J.-R. Proton Conductivities in Functionalized UiO-66: Tuned Properties, Thermogravimetry Mass, and Molecular Simulation Analyses. *Cryst. Growth Des.* **2015**, *15*, 5827−5833.

(22) Yang, F.; Xu, G.; Dou, Y.; Wang, B.; Zhang, H.; Wu, H.; Zhou, W.; Li, J.-R.; Chen, B. A Flexible Metal−Organic Framework with a

High Density of Sulfonic Acid Sites for Proton Conduction. *Nat. Energy* **2017**, *2*, 877−883.
(23) Liu, R.-l.; Wang, D.-Y.; Shi, J.-R.; Li, G. Proton Conductive Metal Sulfonate Frameworks. *Coord. Chem. Rev.* **2021**, *431*, No. 213747.
(24) Hoskins, B. F.; Robson, R. Design and Construction of a New Class of Scaffolding-Like Materials Comprising Infinite Polymeric Frameworks of 3D-Linked Molecular Rods. A Reappraisal of the Zinc Cyanide and Cadmium Cyanide Structures and the Synthesis and Structure of the Diamond-Related Frameworks $[N(CH_3)_4][CuIZnII(CN)_4]$ and CuI[4,4',4'',4'''-tetracyanotetraphenyl-methane]$BF_4 \cdot xC_6H_5NO_2$. *J. Am. Chem. Soc.* **1990**, *112*, 1546−1554.
(25) Wang, Z.; Cohen, S. M. Postsynthetic Covalent Modification of a Neutral Metal−Organic Framework. *J. Am. Chem. Soc.* **2007**, *129*, 12368−12369.
(26) Li, J.; Huang, H.; Xue, W.; Sun, K.; Song, X.; Wu, C.; Nie, L.; Li, Y.; Liu, C.; Pan, Y.; Jiang, H.-L.; Mei, D.; Zhong, C. Self-Adaptive Dual-Metal-Site Pairs in Metal−Organic Frameworks for Selective CO_2 Photoreduction to CH_4. *Nat. Catal.* **2021**, *4*, 719−729.
(27) Pang, J.; Yuan, S.; Qin, J.-S.; Lollar, C. T.; Huang, N.; Li, J.; Wang, Q.; Wu, M.; Yuan, D.; Hong, M.; Zhou, H.-C. Tuning the Ionicity of Stable Metal−Organic Frameworks through Ionic Linker Installation. *J. Am. Chem. Soc.* **2019**, *141*, 3129−3136.
(28) Yin, Z.; Wan, S.; Yang, J.; Kurmoo, M.; Zeng, M.-H. Recent Advances in Post-Synthetic Modification of Metal−Organic Frameworks: New Types and Tandem Reactions. *Coord. Chem. Rev.* **2019**, *378*, 500−512.
(29) Ponomareva, V. G.; Kovalenko, K. A.; Chupakhin, A. P.; Dybtsev, D. N.; Shutova, E. S.; Fedin, V. P. Imparting High Proton Conductivity to a Metal−Organic Framework Material by Controlled Acid Impregnation. *J. Am. Chem. Soc.* **2012**, *134*, 15640−15643.
(30) Bureekaew, S.; Horike, S.; Higuchi, M.; Mizuno, M.; Kawamura, T.; Tanaka, D.; Yanai, N.; Kitagawa, S. One-Dimensional Imidazole Aggregate in Aluminium Porous Coordination Polymers with High Proton Conductivity. *Nat. Mater.* **2009**, *8*, 831−836.
(31) Hurd, J. A.; Vaidhyanathan, R.; Thangadurai, V.; Ratcliffe, C. I.; Moudrakovski, I. L.; Shimizu, G. K. H. Anhydrous Proton Conduction at 150 °C in a Crystalline Metal−Organic Framework. *Nat. Chem.* **2009**, *1*, 705−710.
(32) Xu, Q.; Zhang, X.; Zeng, S.; Bai, L.; Zhang, S. Ionic Liquid Incorporated Metal Organic Framework for High Ionic Conductivity over Extended Temperature Range. *ACS Sustainable Chem. Eng.* **2019**, *7*, 7892−7899.
(33) Phang, W. J.; Jo, H.; Lee, W. R.; Song, J. H.; Yoo, K.; Kim, B. S.; Hong, C. S. Superprotonic Conductivity of a UiO-66 Framework Functionalized with Sulfonic Acid Groups by Facile Postsynthetic Oxidation. *Angew. Chem., Int. Ed.* **2015**, *54*, 5142−5146.
(34) Sarango-Ramírez, M. K.; Lim, D.-W.; Kolokolov, D. I.; Khudozhitkov, A. E.; Stepanov, A. G.; Kitagawa, H. Superprotonic Conductivity in Metal−Organic Framework via Solvent-Free Coordinative Urea Insertion. *J. Am. Chem. Soc.* **2020**, *142*, 6861−6865.
(35) Zhang, F.-M.; Dong, L.-Z.; Qin, J.-S.; Guan, W.; Liu, J.; Li, S.-L.; Lu, M.; Lan, Y.-Q.; Su, Z.-M.; Zhou, H.-C. Effect of Imidazole Arrangements on Proton-Conductivity in Metal−Organic Frameworks. *J. Am. Chem. Soc.* **2017**, *139*, 6183−6189.
(36) Mukhopadhyay, S.; Debgupta, J.; Singh, C.; Sarkar, R.; Basu, O.; Das, S. K. Designing UiO-66-Based Superprotonic Conductor with the Highest Metal−Organic Framework Based Proton Conductivity. *ACS Appl. Mater. Interfaces* **2019**, *11*, 13423−13432.
(37) Liu, S.-S.; Han, Z.; Yang, J.-S.; Huang, S.-Z.; Dong, X.-Y.; Zang, S.-Q. Sulfonic Groups Lined Along Channels of Metal−Organic Frameworks (MOFs) for Super-Proton Conductor. *Inorg. Chem.* **2020**, *59*, 396−402.
(38) Feng, D.; Gu, Z.-Y.; Li, J.-R.; Jiang, H.-L.; Wei, Z.; Zhou, H.-C. Zirconium-Metalloporphyrin PCN-222: Mesoporous Metal−Organic Frameworks with Ultrahigh Stability as Biomimetic Catalysts. *Angew. Chem., Int. Ed.* **2012**, *51*, 10307−10310.
(39) Han, Y.; Li, J.-R.; Xie, Y.-B.; Guo, G. Substitution Reaction in Metal−Organic Frameworks and Metal−Organic Polyhedral. *Chem. Soc. Rev.* **2014**, *43*, 5952−5981.
(40) Jiang, J.; Gándara, F.; Zhang, Y.-B.; Na, K.; Yaghi, O. M.; Klemperer, W. G. Superacidity in Sulfated Metal−Organic Framework-808. *J. Am. Chem. Soc.* **2014**, *136*, 12844−12847.
(41) Peng, Y.; Zhang, Y.; Tan, Q.; Huang, H. Bioinspired Construction of Uranium Ion Trap with Abundant Phosphate Functional Groups. *ACS Appl. Mater. Interfaces* **2021**, *13*, 27049−27056.
(42) Müller, K.; Helfferich, J.; Zhao, F.; Verma, R.; Kanj, A. B.; Meded, V.; Bléger, D.; Wenzel, W.; Heinke, L. Switching the Proton Conduction in Nanoporous, Crystalline Materials by Light. *Adv. Mater.* **2018**, *30*, No. 1706551.
(43) Ramaswamy, P.; Wong, N. E.; Shimizu, G. K. H. MOFs as Proton Conductors − Challenges and Opportunities. *Chem. Soc. Rev.* **2014**, *43*, 5913−5932.

https://doi.org/10.1021/acsaem.1c03852
ACS Appl. Energy Mater. 2022, 5, 3235−3241